Distributed Congestion Management of Distribution Grids under Robust Flexible Buildings Operations

Sarmad Hanif, *Student Member, IEEE*, H. B. Gooi, *Senior Member, IEEE*, Tobias Massier, *Member, IEEE*, Thomas Hamacher, Thomas Reindl.

***Abstract*—Flexible demand side energy and reserve procurement has the potential to improve the overall operation of the grid. However, as argued in previous studies, this flexibility might cause congestion in distribution grids. In this paper, we improve the conventional distribution locational marginal price (DLMP) method, while integrating congestion free energy and reserve provision from buildings in distribution grids. First, robust day-ahead (DA) DLMPs are calculated to account for unmodelled dynamics of flexible loads. Second, using dual decomposition, the data sharing requirements between the aggregator and the distribution system operator (DSO) are minimized. Third, a sensitivity-based real-time (RT) adjustment method is presented to remove conservatism of DA robust DLMPs. Case studies are performed on a benchmark distribution system. The numerical results show that the proposed technique efficiently handles load uncertainties and data sharing requirements, improving the practicality of the conventional DMLP method.**

***Index Terms*—Distributed Congestion Management, Real-time Adjustment, Robust Optimization, Flexible Buildings, Distribution Locational Marginal Pricing (DLMP).**

I. Introduction

Due to their high contribution in greenhouse gas emissions, it is important to operate buildings in a more energy efficient manner [1]. This motivation along with advancements in controllable building models [2]–[4] have spurred researchers in developing energy efficient and grid-friendly building operation strategies [3]–[6]. With similar goals, in our previous work [7]–[10], we presented buildings as a reliable resource for procuring flexible energy and reserve. We showed that flexible operation of buildings can improve their operational cost, while providing consumer satisfaction and grid side reserves. In this paper, we significantly extend our previous works, incorporating methods to account for uncertain flexible demand when integrated in congested distribution grids.

The issue of congestion management due to the introduction of price responsive demand was highlighted in [11]–[13]. One of the main causes for congestion was outlined as a result of the weakening of the correlation between the wholesale electricity price and demand. The authors in [11], [12] provided both a holistic view and quantitative comparisons of various congestion alleviating methods. The work in [13] was more focused towards the comparison of common congestion alleviating solution techniques. Focusing on a particular type of price-based control, the authors in [14]–[16] proposed the concept of DA DLMP to alleviate congestion due to flexible loads. The DLMP method (1) provided the lowest possible theoretical cost to alleviate congestion and (2) was realizable due to its similarity with the existing locational marginal price (LMP) concept at the transmission level. However, while calculating DA DLMPs, the authors in [14]–[16] did not account uncertainties in predicting flexible demand.

Recently, [17] presented a new DLMP method to account for uncertain flexible demand. A sensitivity-based iterative solution was obtained after quantifying the prediction error's probability distribution. However, the proposed method of [17] relied on the DSO to predict uncertain flexible demand. This assumption in our opinion suffers from two major practical drawbacks. First, predicting large scale flexible demand may overburden the operation of the DSO. This is because the DSO is primarily responsible for maintaining/operating the grid and has little or no interest in commercial (maximizing profit) activities. Second, due to modeling complexities and/or privacy concerns, load owners (users) may not be able to share with the DSO, the necessary information required for predicting their demand. Apart from drawback related to data sharing requirements, another important consideration of RT adjustment is also found missing in uncertain DLMP framework of [17]. This consideration is important because methods to mitigate uncertainties cause models to deviate from their deterministic (optimal) behavior [5], [6], [18]. For DLMPs, this deviation would influence the cost of energy delivery to the customer. Since uncertain predictions are much more accurate closer to their actual realization [19], there must exist a method to perform RT or near RT adjustment of uncertain DLMPs. It is also shown from pilot projects [20], [21] that when controlled near RT, flexible loads operate closer to their preferred behavior. Generally, the above mentioned privacy concerns and uncertainty handling techniques are also recognized as one of the major hurdles for realizing smart distributed energy resources in the future grid [22]–[24].

Regarding the above mentioned missing data sharing constraints of the DLMP framework, one can propose a distributed solution technique. These techniques with respect to integrating flexible resources in the grid were reported in [25]–[31]. Recent studies in [25]–[28] proposed methods based on alternating direction method of multipliers (ADMM) [32]. Though these methods provided fast convergence, these works did not consider the restriction of the network and the flexible demand information to the DSO and aggregators, respectively. These

This work was financially supported by the Singapore National Research Foundation under its Campus for Research Excellence And Technological Enterprise (CREATE) programme. This work was also sponsored by National Research Foundation, Prime Ministers Office, Singapore under its Competitive Research Programme (CRP grant NRF2011NRF-CRP003-030, Power grid stability with an increasing share of intermittent renewables (such as solar PV) in Singapore).

works assumed that network information (complex voltage and angle) is also available at the aggregator level to promote a more decentralized solution. However, our focus is to achieve a distributed approach, which promotes coordination of the involved entities while preserving their individual privacy. In [30], [31] some privacy between aggregators and the DSO was considered. Nevertheless, in the proposed methods of [30], [31], the DSO solves an optimization problem. This could cause an increase in the overall computation requirements of the DSO. Another focus of this paper is to consider privacy of uncertain flexible demand in combination with the RT adjustment. According to our knowledge, this has not been addressed in any of the relevant existing literature on distributed solution techniques [25]–[31].

To summarize, the current DLMP framework [14]–[17] suffers from important practical aspects of (i) handling un-modeled dynamics of flexible loads, (ii) minimizing data sharing requirements and (iii) the intra-day (RT) adjustments of the already obtained DA DLMPs. Apart from the above mentioned methodological shortcomings, an implementation consideration found missing in the current DLMP framework is the inclusion of robust operations of buildings.

From the above mentioned deficiencies of the DLMP method, in this paper, we solve (i) and (ii) by forming robust DLMPs and calculating them in a distributed manner. The proposed approach relieves the DSO from predicting the uncertain demand. Resultantly, uncertainties in flexible demand are handled locally (privately) by aggregators. The main reason for locally handling uncertainties is the fact that usually aggregators are commercial and competitive entities. As a result, compared to the DSO, aggregators have a higher motivation to account for un-modeled dynamics of their loads. Moreover, aggregators might also not feel comfortable, sharing their sensitive load data with the DSO. And consistent with the original DLMP framework [14]–[17], we also keep the network information (feeder and line loadings) only to the DSO. Furthermore, in our proposed method the DSO is only assigned to evaluate an inexpensive linear algebraic term, which helps to minimize its overall computation requirements. The deficiency number (iii) is erected using sensitivity-based RT adjustment of the already obtained DA DLMPs. The RT adjustment follows a receding horizon manner, utilizing updated (actual) states of flexible loads and keeping the overall local information handling framework consistent. By addressing the above mentioned deficiencies, this paper not only improves the current DLMP framework, but also presents a novel analysis on handling distributed uncertain flexible demand and its relationship with the RT adjustment.

This paper also significantly extends our previous work in [10]. The major improvements in terms of new formulations and the proposed solution methodologies consist of (1) formulating robust counterparts of DLMPs to account for uncertainties in predicting flexible demand, (2) solving for robust DLMPs using a privacy preserving distributed approach and (3) proposing the RT adjustment solution to account for conservatism of the already obtained robust DA DLMPs. From the major contributions perspective, using a two-step approach, this paper bridges the gap between deterministic and uncertain DLMPs. In doing so, this paper significantly improves the distributed DSO-aggregator cooperation framework of [10] by enabling it to efficiently handle uncertain flexible demand predictions locally.

Section II explains preliminaries for this paper. The proposed robust DA DLMPs with their RT adjustment is in Section III. Section IV presents simulation setup and some key results. Section V provides conclusion and future works.

NOTATIONS

For each zone at time step t (discrete k):

$\hat{d}_t \in \mathbb{R}^{n_{i_d}}$	External and internal disturbances
ρ, Δp, c_{p}	Density of air, pressure difference across the fan, and specific heat capacity of air
τ^i_{ri}, α_{wi}	Transmittance of window i and absorptivity coefficient of wall, respectively
A^i_{ri}, A_{wi}	Total area of window i and total area of the wall wi, respectively
C_{wi}, C_{ri}	Thermal capacitance of wall and room
$n_{b,i}$, n_f, n_r	Number of buildings, floors and rooms
N_{wi}, N_{ri}	The set of all connected nodes to walls and the room, respectively
$p_{\mathrm{heat},k}$, $p_{\mathrm{fan},k}$	Heating and fan power [kW]
$p_k \in \mathbb{R}^{n_{i_r} n_{i_u}}$	Input schedule ([$u_{\mathrm{m},k}$ $r_{\mathrm{m},k}$]') [kg/sec]
$q''_{rad_{ri}}$, $\dot{q}_{int_{ri}}$	Solar radiation and internal heat generation in the room, respectively
r_i	Equal to 0 for internal and 1 for peripheral walls.
$r_{\mathrm{m},k} \in \mathbb{R}^{n_{i_r}}$	HVAC's mass flow reserve schedule [kg/sec]
R_{ij}	Thermal resistance between node i and j
T_{wi}, T_{ri}, T_{si}	Temperature of walls, rooms and HVAC's supply
$u_{m,t} \in \mathbb{R}^{n_{i_u}}$	HVAC's mass flow energy schedule [kg/sec]
wi, ri	number of walls and rooms
$x_t \in \mathbb{R}^n$	Thermal state vector [deg C]

For aggregator i at discrete time step k:

$\hat{\mathbf{d}}_{i,k} \in \mathbb{R}^{n_{d,i}}$	External and internal disturbances
$\mathbf{w}_{i,k} \in \mathbb{R}^{n_{d,i}}$	Disturbance uncertainty
$\mathbf{p}_{i,k} \in \mathbb{R}^{n_{p,i}}$	Input schedule ([$\mathbf{u}_{i,k}$ $\mathbf{r}_{i,k}$]')
$\mathbf{x}_{i,k} \in \mathbb{R}^{n_{x,i}}$	Thermal states
n, n_{i_u}, n_{i_d}	Number of states, HVACs and disturbances
$n_{x,i}$, $n_{d,i}$, $n_{p,i}$	Number of states ($n_{b,i}{\cdot}n_f{\cdot}n_r{\cdot}n$), disturbances ($n_{b,i}{\cdot}n_f{\cdot}n_r{\cdot}n_{i_d}$) and inputs ($n_{b,i}{\cdot}n_f n_r{\cdot}n_{i_u}{\cdot}n_{i_r}$)

For modeling market:

β	Price sensitivity coefficient [\$/(kWh)^2]
$c_{0,k}$	Baseline price [\$/kWh]
z_k	Reserve price [\$/kWh]

II. Preliminaries

A. Zone Model

To predict building dynamics, a resistance-capacitance (R-C) based zone modeling is deployed [1]. The zone models are then aggregated to obtain the thermal model of the whole building. A variable frequency drive fan based HVAC system is considered as a source of flexibility in the modeled zone of each building. In principle, by modulating the fan speed, the energy consumption as well as the temperature of the room is controlled. An R-C (lumped) model of a zone contains thermal resistances and capacitances, representing heat transfer and heat storage, respectively. The differential equations governing temperature evolutions of walls and room become:

$$\frac{dT_{wi}}{dt} = \frac{1}{C_{wi}}\left[\sum_{j\in N_{wi}} \frac{T_j - T_{wi}}{R_{ij}} + r_i \alpha_{wi} A_{wi} q''_{rad_{ri}}\right], \quad (1a)$$

$$\frac{dT_{ri}}{dt} = \frac{1}{C_{ri}}\left[\sum_{j\in N_{ri}} \frac{T_j - T_{ri}}{R_{ij}} + \dot{m}_{ri} c_p \left(T_{si} - T_{ri}\right) + w_i \tau^i_{ri} A^i_{ri} q''_{rad_{ri}} + \dot{q}_{int}\right]. \quad (1b)$$

Details regarding units and parameters of the R-C model with the method to translate them from physical quantities to state-space models is given in [1]. The nonlinear relationship of temperature of the zone x_t with the HVAC mass flow rate $u_{\mathrm{m},t}$ can be generalized as:

$$\dot{x}_t = Ax_t + g(x_t, u_{\mathrm{m},t}) + \hat{d}_t. \quad (2)$$

The expression in (2) is of nonlinear nature. Since the most efficient controllers are obtained for linear systems, the nonlinear model described above is linearized and discretized using sequential quadratic programing and zero order hold, respectively [33]. In [33], it is shown that linearizing around the usual operating point does not introduce significant errors. This is mainly because the temperature range of the building is normally not very large. The resultant discrete time linear system at step k is:

$$\begin{aligned} x_{k+1} &= Ax_k + B_{\mathrm{u}} u_{\mathrm{m},k} + E\hat{d}_k + B_{\mathrm{r}} r_{\mathrm{m},k}, \\ x_{k+1} &= Ax_k + B_{\mathrm{agg}} p_k + E\hat{d}_k. \end{aligned} \quad (3)$$

In (3), $p_k = [u_{\mathrm{m},k}\ r_{\mathrm{m},k}]'$ is used to compactly represent usual energy and reserve consumption variables. Matrices A, B_{agg} and E are of the appropriate sizes. Correspondingly, the electrical power consumed for heating $p_{\mathrm{heat},t}$ and fan $p_{\mathrm{fan},t}$ is given as:

$$p_{\mathrm{heat},t}(u_{\mathrm{m},t}) = u_{\mathrm{m},t} c_{\mathrm{p}} (T_{si} - T_{ri}), \quad (4a)$$

$$p_{\mathrm{fan},t}(u_{\mathrm{m},t}) = \frac{u_{\mathrm{m},t}\Delta p}{\rho}. \quad (4b)$$

The building model described above is simple, yet it provides physical interpretation of all of its underlying variables. This property can be easily exploited to rapidly translate this model to the form used by state-of-the-art building modeling tools [34]–[36]. In [10], we showed an example to achieve this translation for the above described building model.

B. Aggregator Model

The aggregator is responsible for procuring flexibility for its contracted buildings. The aggregator i augments the zonal model of (3) to predict thermal states as:

$$\mathbf{x}_{i,k} = \mathbf{A}x_{i,0} + \mathbf{B}_{\mathrm{agg}}\mathbf{p}_{i,k} + \mathbf{E}\hat{\mathbf{d}}_{i,k} \quad (5)$$

In this paper, a liberalized market setting is assumed which allows loads to bid for reserves and energy provision through the interruptible load (IL) [37] and the demand response [38] program, respectively. Practical examples of these programs can be found in the National Electricity Market of Singapore [39]. In the IL program, aggregators need to reserve some of its load. If required, this load is curtailed by the system operator. Hence, to account for system operator's decision to curtail or not, the aggregator must predict both curtailed and not-curtailed temperature trajectories,

$$\mathbf{x}^{nc}_{i,k+1} = \mathbf{A}\mathbf{x}^{nc}_{i,k} + \mathbf{B}^{nc}_{\mathrm{agg}}\mathbf{p}_{i,k} + \mathbf{E}\hat{\mathbf{d}}_{i,k}, \quad (6a)$$

$$\mathbf{x}^{c}_{i,k+1} = \mathbf{A}\mathbf{x}^{nc}_{i,k} + \mathbf{B}^{c}_{\mathrm{agg}}\mathbf{p}_{i,k} + \mathbf{E}\hat{\mathbf{d}}_{i,k}. \quad (6b)$$

Matrices $\mathbf{B}^{nc}_{\mathrm{agg}}$ and $\mathbf{B}^{c}_{\mathrm{agg}}$ in (6a) and (6b) differentiate between the not-curtailed and curtailed consumptions, respectively. The not-curtailed trajectory (6a) is similar to (5), as the original prediction model (5) already contains both the usual energy and reserve consumption variables. The curtailed trajectory is predicted by placing zeros at positions of $\mathbf{B}^{c}_{\mathrm{agg}}$, which corresponds to the reserve vector ($\mathbf{r}_{i,k}$). This ensures that the curtailed trajectory has a maximum deviation from the not-curtailed one i.e. full curtailment of the offered load at step k ($\mathbf{r}_{i,k}$ = **0**). This maximum deviation is then captured in the model by using only the not-curtailed trajectory at step k to predict both the not-curtailed (6a) and curtailed trajectories (6b) for step $k+1$. This couples both the not-curtailed and curtailed trajectories in the aggregator model, necessitating co-optimization of both reserves and energy.

1) Co-optimizing Energy and Reserve Schedule: In this paper, it is assumed that the aggregator similar to its users shares the same objectives of minimizing the total cost of energy procurement. The total cost $J_{sum_{i,k}}$ for procuring energy and reserves by aggregator i is then:

$$J_{sum_{i,k}} = J_{u_{\mathrm{m}_{i,k}}} + J_{r_{\mathrm{m}_{i,k}}} - R_{r_{\mathrm{m}_{i,k}}}, \quad (7)$$

where $J_{u_{\mathrm{m}}/r_{\mathrm{m}_{i,k}}}$ and $R_{r_{\mathrm{m}_{i,k}}}$ are the cost of energy/reserves consumption and the revenue due to the allocation of reserves. Since the global convergence for DLMPs [16] only holds true for QPs, we are also going to consider quadratic cost formulation. This is achieved by assuming correlation of demand d_k with the spot price y_k, through a price sensitivity coefficient β [11],

$$y_k = c_{0,k} + \beta d_k. \quad (8)$$

The procedure for obtaining values of β and $c_{0,k}$ is explained in [11]. Using (8), the cost of consuming energy and placing reserves for a constant time interval Δt becomes:

$$\begin{aligned} J_{u_{\mathrm{m}_{i,k}}} &= y_k p(u_{\mathrm{m},k})\Delta t \\ &= c_{0,k} p(u_{\mathrm{m},k})\Delta t + \beta (p(u_{\mathrm{m},k})\Delta t)^2 \\ J_{r_{\mathrm{m}_{i,k}}} &= c_{0,k} p(r_{\mathrm{m},k})\Delta t + \beta (p(r_{\mathrm{m},k})\Delta t)^2 \end{aligned} \tag{9}$$

with $p(u_{\mathrm{m},k}/r_{\mathrm{m},k}) = p_{\mathrm{heat},k}(u_{\mathrm{m},k}/r_{\mathrm{m},k}) + p_{\mathrm{fan},k}(u_{\mathrm{m},k}/r_{\mathrm{m},k})$. In order to calculate the revenue from placing reserves under the IL program, we consider the market setting of ILs getting paid based on their availability[1] and presence in the respective reserve groups[2]. Due to thermal inertia, buildings can rapidly vary their power consumption without much loss in comfort constraints. Hence, we propose to use maximum reserve prices z_k, as cleared in the market, to schedule and calculate revenue from reserves[3] as:

$$R_{r_{\mathrm{m}_{i,k}}} = z_k p(r_{\mathrm{m},k})\Delta t \tag{10}$$

For constant time interval Δt and conversion factors (see Section II-A), substituting (9) – (10) in (7), the total cost for one zone becomes:

$$J_{sum_k} = c_k^T p_k + \frac{1}{2} p_k^T B p_k \tag{11}$$

with,

$$c_k = \begin{bmatrix} c_{0,k} \\ c_{0,k} - z_k \end{bmatrix}, \; B = \begin{bmatrix} \beta & 0 \\ 0 & \beta \end{bmatrix}, \tag{12}$$

Similarly, for aggregator i, the total cost at time step k becomes:

$$\mathbf{J}_{sum_{i,k}} = \mathbf{c}_k^{\mathbf{T}} \mathbf{p}_{i,k} + \frac{1}{2} \mathbf{p}_{i,k}^{\mathbf{T}} \mathbf{B} \mathbf{p}_{i,k}. \tag{13}$$

Here, $\mathbf{c}_k \in \mathbb{R}^{n_{p,i}}$ and $\mathbf{B} \in \mathbb{R}^{n_{p,i} \times n_{p,i}}$ are the augmented and block diagonal versions of c_k and B, respectively. For both curtailed (6a) and not-curtailed (6b) trajectories, (13) represents the overall cost for purchasing energy and placing reserves by the aggregator. Note that when calculating cost (13), variables $p(u_{\mathrm{m},k})$ and $p(r_{\mathrm{m},k})$ and their augmented vector $\mathbf{p}_{i,k}$ are internally converted to have units of kW.[4]

C. DLMP Method

The authors in [14]–[16] proposed the DA dynamic tariff based DLMP method to alleviate congestion in distribution grids. This procedure is summarized as follows:

1) With the knowledge of network data, the DSO predicts load and market data to calculate DLMPs, which adhere to its grid limitations.
2) The aggregators after receiving DLMPs incorporate them into their energy planning.
3) Finally, the aggregators submit their optimized energy plan to the spot market.

For the optimal congestion alleviation using DLMPs, the above mentioned method is carried out by formulating the DSO and aggregator problems as QPs [16], [17]. This formulation is only possible with the assumption of DC power flowing across the network. This means that voltage profiles of the network are assumed to be flat (1 per unit) and losses are ignored. Since the focus of this paper is towards the improvement of data sharing requirements and the uncertainty handling capabilities of the current DLMP framework [16], [17], we also proceed with the DC power flow.

The DSO problem for the scope of this paper is then represented as:

$$\min_{\mathbf{p}^*_{i,k}} \sum_{i \in N_i} \sum_{k \in N_t} \mathbf{J}_{sum_{i,k}} \tag{14a}$$

subject to

$$-f_l \leq \sum_{i \in N_i} \sum_{k \in N_t} DM_i \mathbf{p}_{i,k} \leq f_l \;\; (\lambda_k^{DA^-}, \lambda_k^{DA^+}) \tag{14b}$$

$$\mathbf{x}^c_{i,k+1} = \mathbf{A}\mathbf{x}^{nc}_{i,k} + \mathbf{B}^c_{\mathrm{agg}} \mathbf{p}_{i,k} + \mathbf{E}\hat{\mathbf{d}}_{i,k} \tag{14c}$$

$$\mathbf{x}^{nc}_{i,k+1} = \mathbf{A}\mathbf{x}^{nc}_{i,k} + \mathbf{B}^{nc}_{\mathrm{agg}} \mathbf{p}_{i,k} + \mathbf{E}\hat{\mathbf{d}}_{i,k} \tag{14d}$$

$$\mathbf{x}^{min}_{i,k} \leq \mathbf{x}^c_{i,k} \leq \mathbf{x}^{max}_{i,k} \tag{14e}$$

$$\mathbf{x}^{min}_{i,k} \leq \mathbf{x}^{nc}_{i,k} \leq \mathbf{x}^{max}_{i,k} \tag{14f}$$

$$\mathbf{u}^{min}_{i,k} \leq \mathbf{A}^{\mathrm{sum}} \mathbf{p}_{i,k} \leq \mathbf{u}^{max}_{i,k} \tag{14g}$$

$$\mathbf{p}_{i,k}, \mathbf{A}^{\mathrm{diff}} \mathbf{p}_{i,k} \geq \mathbf{0} \qquad \forall i \in N_i, \forall k \in N_t \tag{14h}$$

In the above DSO problem, N_i and N_t are the total number of aggregators and time duration respectively. The output of (14) is the optimal input sequence $\mathbf{p}^*_{i,k}$ for all aggregators. Note that in this context, optimality is in terms of minimizing the total cost of the system while satisfying network and user constraints. Using (14g) and (14h), the actuator limits of all HVAC systems are constrained. Matrices $\mathbf{A}^{\mathrm{sum}}$ and $\mathbf{A}^{\mathrm{diff}}$ ($\in \mathbb{R}^{n_b \cdot n_{br} \cdot n_{i_u} \times n_{p,i}}$) contain vectors [1 1] and [1 -1] at appropriate entries to compactly represent addition and subtraction of $u_{\mathrm{m},k}$ and $r_{\mathrm{m},k}$ variables of each zone. Both curtailed (14c) and not-curtailed (14d) temperature trajectories are kept feasible through (14e) and (14f), respectively. If distribution grid contains n_{LP} load points (LPs) and n_l distribution lines, then $D \in \mathbb{R}^{n_l \times n_{LP}}$ represents power transfer distribution factor (PTDF). Matrix $M_i \in \mathbf{R}^{n_{LP} \times n_{p,i}}$ converts the combined energy and reserve vectors of the aggregators contained in $\mathbf{p}_{i,k}$ to the total power at corresponding LPs of the grid.[5]. The Lagrange multipliers (LMs) $\lambda_k^{DA}(\lambda_k^{DA^+} - \lambda_k^{DA^-}) \in \mathbb{R}^{n_l})$ represent sensitivity of binding line limits $f_l \in \mathbb{R}^{n_l}$ in (14b). For time k and aggregator i, if the partial Lagrangian of (14) with only binding line limits is:

$$L(\mathbf{p}_{i,k}, \lambda_k^{DA}) = \mathbf{J}_{sum_{i,k}} + \lambda_k^{DA^T}(DM_i \mathbf{p}_{i,k} - f_l). \tag{15}$$

[1]Modeling activation of reserves based on the spot market operation is out of the scope of this paper.

[2]The reserve groups represent their member's response time and output quality [40].

[3]From market perspective this means that the reserve provision from buildings is placed in the highest quality reserve group of the market clearing engine. This assumption is not far from reality. As in [39], it has also been mentioned that loads, compared to generators, possess a natural advantage when providing reserves.

[4]This is done to keep the notation light and easy to follow. In principle, the conversion from mass flows in kg/s to kW can be simply done using (4).

[5]This is done by summing up both usual energy and reserve vectors of the corresponding aggregators and converting their units from kg/s to kW using (4).

Then DLMPs ($\lambda_{\mathrm{dlmp}_{i,k}}$) with units \$/kWh are defined as:

$$\lambda_{\mathrm{dlmp}_{i,k}} = \frac{\partial L}{\partial \mathbf{p}_{i,k}} = \mathbf{c} + \mathbf{B}\mathbf{p}_{i,k} + \lambda_k^{DA^T} DM_i. \qquad (16)$$

From (16), it can be seen that DLMPs consists of two components: (1) the (predicted) market data and (2) the distribution line conditions. Consequently, it can be stated that the current DLMP framework only attempts to reflect congestion in the energy planning (cost optimization) of aggregators. It must be noted that to form a distribution grid market mechanism using these DLMPs, a more rigorous analysis of these DLMPs is required. In [10], [17], some possible regulatory and settlement arrangements regarding the collected revenue from DLMPs are discussed. Since, the focus of this paper is towards uncertainty handling, the design of a market layer on top of DLMPs is not considered.

Aggregator i after receiving DLMPs from the DSO, obtains its final energy plan as:

$$\min_{\mathbf{p}^*_{i,k}} \sum_{k\in N_t} \lambda^T_{\mathrm{dlmp}_{i,k}} \mathbf{p}_{i,k} + \frac{1}{2}\mathbf{p}^{\mathbf{T}}_{\mathrm{i},k}\mathbf{B}\mathbf{p}_{\mathrm{i},k} \qquad (17)$$
subject to
(14c) – (14h) $\qquad \forall k \in N_t$

Under deterministic settings and strictly convex (QP) formulations, both aggregators (17) and the DSO (14) solutions converge to a unique solution [16].

Table I
COMPARISON OF DATA REQUIREMENTS BETWEEN CONVENTIONAL (*A*) AND PROPOSED METHOD (*B*)

Entity	Load Data		Market Data		Network Data	
	A	*B*	*A*	*B*	*A*	*B*
DSO	✓	×	✓	×	✓	✓
Aggregator	✓	✓	✓	✓	×	×

Load Data: parameters for flexible loads models, Market Data: energy, reserve and sensitivity price
Network Data: Distribution grid lines, limitations and inflexible (base) loads

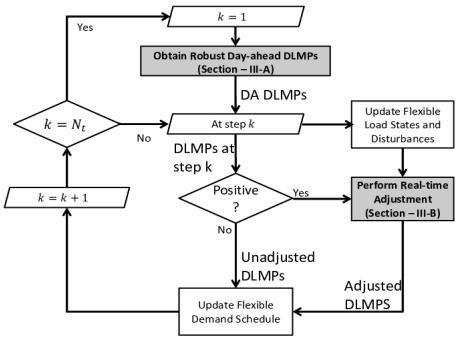

Fig. 1. Flow chart of the proposed method. See Fig. 3 and Fig. 4 for more information regarding DA DLMP and RT adjustment procedures respectively. This flow chart shows the generic organization of the whole procedure. Note that the exact timing for running the proposed methods will depend on predefined market rules.

III. DISTRIBUTED ROBUST CONGESTION ALLEVIATION

As motivated earlier, the DSO should be relieved of the duty to estimate energy consumption of its underlying uncertain loads. In this section, we propose a method to alleviate congestion due to consumption from uncertain flexible buildings in a distributed manner. The proposed method achieves this in two steps: (1) calculating robust DA DLMPs and (2) applying RT adjustment.

Both steps, calculating DA DLMPs and their RT adjustment, are carried out in a distributed manner. The term distributed here refers to handling local information privately. This means that sensitive information (load/network data) is only processed by the corresponding local entity (aggregators/DSO) to obtain local solutions[6]. These local solutions are then coordinated between the DSO and aggregators to obtain the final solution. It must be noted here that the coordination procedure to arrive at the final procedure is however different for both steps. For DA DLMPs, we propose an iterative procedure (Section III-A2), and for the RT adjustment we design a clearing method (Section III-B2) for sensitivity-based locally calculated demand bids (Section III-B1).

Compared to the conventional DLMP methods, Table I presents the improvement in the data requirements from the proposed method. Note that in the proposed method of this paper the DSO never estimates any load and/or market data. Also, the proposed method does not require any additional data requirements as compared to the conventional DLMP method. The Flow chart depicting the overall working of the proposed method is presented in Fig. 1.

A. Robust Day-ahead DLMPs

The pictorial representation of the proposed method is given in Fig. 3. Note that in this method for computing DLMPs, only prices are iterated between aggregators and the DSO. Hence, the local information of the DSO (grid data) and aggregators (load data) are kept completely private. Furthermore, aggregators are only operating within bounded load dynamics, to account for disturbance uncertainties.

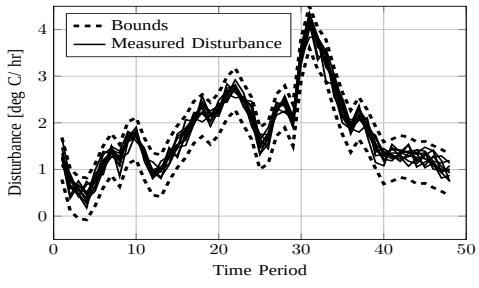

Fig. 2. Measured disturbances of the zonal model [18].

1) Uncertainties in Disturbance: The zonal model described in (3) experiences both external and internal disturbances. As seen from (1), there exists two disturbance sources: (i) external disturbances, experienced due to solar radiation $q''_{rad_{ri}}$ and (ii) internal disturbances, caused by electronic

[6]This local data handling for both methods can be clearly observed in Fig. 3 and Fig. 4 for DA DLMPs and RT adjustment methods respectively.

components and occupancy $\dot{q}_{int}$. Even though it is extremely hard to predict the actual probability distribution to estimate these disturbances, their worst-case bounds can readily be obtained by observing historical data [18] (See Fig. 2). If w_k is a stochastic disturbance entering the zonal model additively,

$$x_{k+1} = Ax_k + B_{\text{agg}}p_k + E(\hat{d}_k + w_k), \tag{18}$$

then we assume $w_k \in \mathcal{W}$ to be bounded. The polyhedral set $\mathcal{W} = \{w_k : \|w_k\|_\infty \leq \sigma_k\}$ represents a box-constrained disturbance uncertainties set. The bounded values represented by σ_k can be considered as l_∞ norm bound of the observed uncertainty. The two main advantages of representing disturbance as a polyhedral set $\mathcal{W}$ are: (1) it is easily realizable from historical data [18], and (2) it helps in preserving the structure of the optimization problem. Similar to (18), aggregators can use the augmented version of (6) as:

$$\mathbf{x}^c_{i,k+1} = \mathbf{A}\mathbf{x}^{nc}_{i,k} + \mathbf{B}^c_{\text{agg}}\mathbf{p}_{i,k} + \mathbf{E}(\hat{\mathbf{d}}_{i,k} + \mathbf{w}_{i,k}) \tag{19}$$

$$\mathbf{x}^{nc}_{i,k+1} = \mathbf{A}\mathbf{x}^{nc}_{i,k} + \mathbf{B}^{nc}_{\text{agg}}\mathbf{p}_{i,k} + \mathbf{E}(\hat{\mathbf{d}}_{i,k} + \mathbf{w}_{i,k}) \tag{20}$$

Uncertainties Robustification: The polyhedral disturbance set of Section III-A1 is included in the optimization framework of aggregators by forming the robust counterparts of [(19), (20)]. This can be achieved by forming the dual of these constraints. Consider the uncertain curtailed states update equation of (19)[7]:

$$\max_{\mathbf{w}_{i,k}\in\mathcal{W}} \mathbf{x}^c_{i,k+1} = \mathbf{A}\mathbf{x}^{nc}_{i,k} + \mathbf{B}^c_{\text{agg}}\mathbf{p}_{i,k} + \mathbf{E}(\hat{\mathbf{d}}_{i,k} + \mathbf{w}_{i,k}). \tag{21}$$

The uncertain part of (21) can be separated as:

$$\max_{\mathbf{w}_{i,k}} \quad \mathbf{E}\mathbf{w}_{i,k} \tag{22a}$$

$$\text{s.t.} \quad \mathbf{w}_{i,k} \leq \boldsymbol{\sigma}_{i,k} \ (\boldsymbol{\lambda}^+_{w_{i,k}}) \tag{22b}$$

$$-\mathbf{w}_{i,k} \leq \boldsymbol{\sigma}_{i,k} \ (\boldsymbol{\lambda}^-_{w_{i,k}}) \quad \forall i \in N_i, \forall k \in N_t, \tag{22c}$$

and replaced by its associated dual,

$$\min_{\boldsymbol{\lambda}^+_{w_{i,k}}, \boldsymbol{\lambda}^-_{w_{i,k}}} \quad \boldsymbol{\lambda}^+_{w_{i,k}}\boldsymbol{\sigma}_{i,k} + \boldsymbol{\lambda}^-_{w_{i,k}}\boldsymbol{\sigma}_{i,k} \tag{23a}$$

$$\text{s.t.} \quad \boldsymbol{\lambda}^+_{w_{i,k}} - \boldsymbol{\lambda}^-_{w_{i,k}} = \mathbf{E} \tag{23b}$$

$$\boldsymbol{\lambda}^+_{w_{i,k}}, \boldsymbol{\lambda}^-_{w_{i,k}} \geq \mathbf{0} \quad \forall i \in N_i, \forall k \in N_t. \tag{23c}$$

By duality, any feasible ($\boldsymbol{\lambda}^+_{w_{i,k}}$, $\boldsymbol{\lambda}^-_{w_{i,k}}$) in (23) will be the upper bound for the maximization of (22). Hence, we can drop the minimization term in (23) and due to strong duality in linear programming [41] the achieved solution for both primal and dual will be the same. The robust counterpart of the original aggregator problem can then be completed by including [(23a) – (23c)] in (17). The final robust counterparts for aggregators and the DSO problem are shown in Section VI-A. Section VI-B presents the global convergence proof for the robust DSO and aggregators problems.

The global optimality proof in Section VI-B shows that the robust solution, accounting for the worst-case disturbances, is unique for both the DSO and aggregators. Essentially, this means that the DSO must deploy identical polyhedral sets as aggregators for calculating its robust DLMPs. In the next subsection, we relieve the DSO from predicting any disturbance sets by proposing an iterative-based solution technique.

[7]The robust counterpart of the not-curtailed constraint (20) follows exactly the similar procedure.

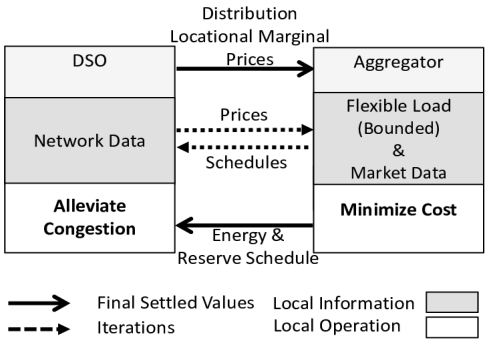

Fig. 3. The coordination between the DSO and the aggregator for calculating distributed DA DLMPs. The DSO only passes LMs (prices) connected to (14b).

2) Iterative-based Distributed DLMPs: The price iterations shown in Fig. 3 are achieved by decomposing the original problem into the respective independent subproblems. In general, this decomposition is obtained by exploiting partial duality (dual of partial constraints) of the original problem. The partial LMs then serve as coordination variables between the master (DSO) and local subproblems (aggregators). Also in this paper, the coupling constraint between the local subproblems and the DSO problem is given by (14b). Consider the Lagrangian of the robustifed DSO problem (36) with constraints only related to the input vector $\mathbf{p}_{i,k}$:

$$\begin{aligned} L(\mathbf{p}_{i,k}, \lambda_k^{DA^+}, \lambda_k^{DA^-}, \nu^c_{i,k}, \nu^{nc}_{i,k}, \mu^{+\text{sum}}_{i,k}, \mu^{-\text{sum}}_{i,k}, \mu^{\text{diff}}_{i,k}, \mu^{\mathbf{p}_{i,k}}_{i,k}) = \\ \sum_{i\in N_i}\sum_{k\in N_t} \mathbf{J}_{sum_{i,k}} + ((\lambda_k^{DA^+} - \lambda_k^{DA^-})^T(DM_i\mathbf{p}_{i,k} - f_l)) \\ + \nu^{c^T}_{i,k}(-\mathbf{x}^c_{i,k+1} + \mathbf{A}\mathbf{x}^{nc}_{i,k} + \mathbf{B}^c_{\text{agg}}\mathbf{p}_{i,k} + \mathbf{E}\hat{\mathbf{d}}_{i,k} + \boldsymbol{\lambda}^+_{w_{i,k}}\boldsymbol{\sigma}_{i,k} \\ + \boldsymbol{\lambda}^-_{w_{i,k}}\boldsymbol{\sigma}_{i,k}) + \nu^{nc^T}_{i,k}(\mathbf{x}^{nc}_{i,k+1} - \mathbf{A}\mathbf{x}^{nc}_{i,k} + \mathbf{B}^{nc}_{\text{agg}}\mathbf{p}_{i,k} + \mathbf{E}\hat{\mathbf{d}}_{i,k} \\ + \boldsymbol{\lambda}^+_{w_{i,k}}\boldsymbol{\sigma}_{i,k} + \boldsymbol{\lambda}^-_{w_{i,k}}\boldsymbol{\sigma}_{i,k}) + \mu^{+\text{sum}^T}_{i,k}(\mathbf{A}^{\text{sum}}\mathbf{p}_{i,k} - \mathbf{u}^{max}_{i,k}) \\ - \mu^{\mathbf{p}^T_{i,k}}_{i,k}\mathbf{p}_{i,k} + \mu^{-\text{sum}^T}_{i,k}(-\mathbf{A}^{\text{sum}}\mathbf{p}_{i,k} + \mathbf{u}^{min}_{i,k}) - \mu^{\text{diff}^T}_{i,k}\mathbf{A}^{\text{diff}}\mathbf{p}_{i,k} \end{aligned} \tag{24}$$

The Lagrangian above shows that all aggregator's equality ($\nu^c_{i,k}$, $\nu^{nc}_{i,k} \in \mathbb{R}^{n_{x,i}}$) and inequality ($\mu^{+\text{sum}}_{i,k}$, $\mu^{-\text{sum}}_{i,k}$, $\mu^{\text{diff}}_{i,k}$, $\mu^{\mathbf{p}_{i,k}}_{i,k} \in \mathbb{R}^{n_{p,i}}$) LMs are local, except the ones connected to constraint (14b) i.e. λ_k^{DA}. From the Lagrangian above, it must also be noticed that the robustification constraints (23) are only local to each aggregator's underlying prediction model. Therefore, by distributing and coordinating the calculation of these global LMs, we can relieve the DSO from predicting uncertainty disturbance sets. This distributed solution technique is achieved through dual decomposition, decomposing the robust counterpart of the DSO problem (35) into i independent aggregator subproblems (36). The partial LMs of (14b) are evaluated using a projected subgradient algorithm [42]. At time step k and aggregator i, consider the partial Lagrangian of the DSO problem (14),

$$L(\mathbf{p}_{i,k}, \lambda_k^{DA}) = \sum_{k\in N_t} \mathbf{J}_{sum_{i,k}} + \lambda_k^{DA^T}(DM_i\mathbf{p}_{i,k} - f_l), \tag{25}$$

then the dual of the above Lagrangian is represented as:

$$g(\lambda_k^{DA}) = \inf_{\mathbf{p}_{i,k}} L(\mathbf{p}_{i,k}, \lambda_k^{DA}). \tag{26}$$

Using (26) and (25), and excluding the constant term $(-\lambda_k^{DA^T} f_l)$, we get the evaluation of the dual,

$$g(\lambda_k^{DA}) = \inf_{\mathbf{p}_{i,k}} \sum_{k \in N_t} \mathbf{J}_{sum_{i,k}} + \lambda_k^{DA^T}(DM_i \mathbf{p}_{i,k}). \tag{27}$$

Since the structure of problem is convex, the dual function is concave and it can be solved using the sub-gradient method. The subgradient S_k of the negative of the dual $\partial(-g)(\lambda_k^{DA}) \in \mathbb{R}^{n_l}$ becomes,

$$S_k = \sum_{k \in N_t} (DM_i \mathbf{p}_{i,k}^*) - f_l, \tag{28}$$

with $\mathbf{p}_{i,k}^*$ being the solution of the following problem,

$$\min_{\mathbf{p}_{i,k}^*} \sum_{k \in N_t} \lambda_{\text{idlmp}_{i,k}}^T \mathbf{p}_{i,k} + \frac{1}{2} \mathbf{p}_{i,k}^{\mathbf{T}} \mathbf{B} \mathbf{p}_{i,k} \tag{29}$$

subject to

(35c) – (35i) $\quad \forall k \in N_t.$

Compared to $\lambda_{\text{dlmp}_{i,k}}$ in (36), the $\lambda_{\text{idlmp}_{i,k}}$ is computed iteratively and independently by aggregators, using a dual sub-gradient method, outlined below:

1) The DSO initializes the global LMs as: $\lambda_k^{DA} \geq \mathbf{0}$, and publishes $\lambda_{\text{idlmp}_{i,k}}$ to each aggregator using the procedure described in Section II-C.
2) Repeat
   a) Each aggregator i independently solves (29) and obtains the schedule $\mathbf{p}_{i,k}^*$, which is submitted to the DSO
   b) Using (28), the DSO evaluates line limit violations
   c) Based on line limit violations, the global LMs are updated: $\lambda_k^{DA} = (\lambda_k^{DA} + \alpha_k S_k)_+$
3) The procedure is terminated when line loading tolerance is attained or improvement in the dual objective stops.

For the choice of $\alpha_k \in \mathbb{R}_+$, due to (26) being differentiable, it can be chosen as a small positive constant step size to guarantee the convergence [42]. More analysis on the projected sub-gradient method adopted in this paper is presented in Section VI-C. For the final schedule obtained $\mathbf{p}_{i,k}^*$, the cost for the aggregator $g(i)_{sum}$ can be calculated as:

$$\begin{aligned} g(i)_{sum} &= g(i)_{sch} + g(i)_{con} \\ g(i)_{sch} &= \sum_{k \in N_t} \mathbf{c}_k^{\mathbf{T}} \mathbf{p}_{i,k}^* + \frac{1}{2} \mathbf{p}_{i,k}^{*\mathbf{T}} \mathbf{B} \mathbf{p}_{i,k}^* \\ g(i)_{con} &= \sum_{k \in N_t} \lambda_k^{*DA^T}(DM_i \mathbf{p}_{i,k}^*) \end{aligned} \tag{30}$$

where $g(i)_{sch}$ and $g(i)_{con}$ represent the cost for net energy procurement and the congestion contribution by the aggregator i in the network. The distributed method proposed above relieves the DSO from predicting any uncertainties in its demand. Since the above mentioned method adopts worst-case disturbance sets for obtaining robust DA DLMPs, it might suffer from conservatism [18], [19]. This means that flexible loads, compared to their true contribution, when operated under these DLMPs might experience higher congestion cost.

B. Real-time Adjustment

The conservatism of robust solution and its relation to the LMs of the coupling constraint (14b) can be analyzed using a simple QP,

$$\min_{p^*} \frac{1}{2} p^2, \quad \text{s.t. } p \geq e. \tag{31}$$

The above QP is only constrained through minimum energy requirement e for the load p. Intuitively, the above problem has a trivial minimum, given by $p^* = e$. This solution shows that minimum effort to satisfy the load is at its minimum allowed energy requirements. Analytically, this can be shown as,

$$\begin{aligned} &L(p, \lambda) = \frac{1}{2} p^2 + \lambda(e - p), \\ &\frac{\partial(L(p,\lambda))}{\partial p}\Big|_{p=p^*, \lambda=\lambda^*} = 0, \qquad \lambda^* = p^*, \\ &\frac{\partial(L(p,\lambda))}{\partial \lambda}\Big|_{p=p^*, \lambda=\lambda^*} = 0, \qquad e = p^*. \end{aligned} \tag{32}$$

The above solution shows that the LM (of binding constraint) is directly proportional to the strictness of the system. This means a higher energy requirement increases the value of the LM. In Section III-A1, we adopted worst-case bounds to mitigate uncertain disturbances of flexible demand. By comparing aggregator's deterministic (17) and robust counterparts (36), it can be observed that additional positive terms are included by the aggregator to account for worst-case disturbance sets. This means that robust counterparts predict higher energy requirements $\bar{e}$, i.e. $\bar{e} \geq e$. Similarly for the robust LM $\bar{\lambda}$, this translates to $\bar{\lambda} \geq \lambda$. Consequently, the robust LM ($\bar{\lambda}$) may over-constrain flexible loads, when operating under any realized disturbance other than the worst case. Hence, there must exist a procedure to counteract conservatism of the already obtained robust DA DLMPs.

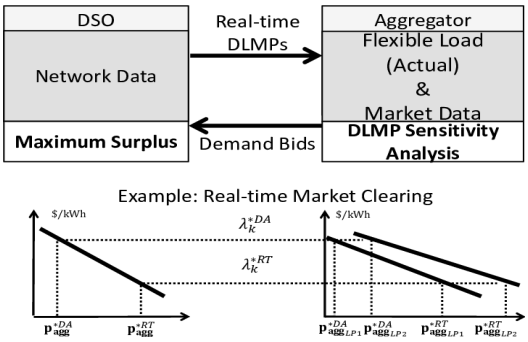

Fig. 4. The information flow required for the RT adjustment (top). An example of the RT market clearing by the DSO using aggregator 1's demand bids (bottom left) and its translation to individual LPs' demand bids (bottom right). Note that the local and global information sharing is consistent with the DA DLMPs (see Fig. 3).

The proposed RT adjustment method is implemented near RT in a receding horizon fashion. This means that DLMPs, adjusted at step k, are used to update thermal states and actuators for step k+1. From Fig. 4, it can be seen that the RT DLMP method maintains the data privacy of aggregators/loads. This is consistent with the distributed philosophy

of our previously presented robust DA DLMP method. Furthermore, by deploying a sensitivity analysis method, local information/calculations are handled locally by aggregators and no iterations are performed with the DSO. Indeed, due to the unknown number of exact iterations to reach the optimal solution (see Section III-A2), the iterative method is not suitable for implementation in a RT. The RT adjustment method essentially operates in two steps: (1) each aggregator forms demand bids using the sensitivity analysis of its respective DA DLMPs and (2) the DSO then uses these demand bids to adjust DA DLMPs (see Fig. 4).

1) DLMP Sensitivity Analysis: The DLMP sensitivity analysis (SA) provides information regarding the flexibility of contracted loads of aggregators with respect to their thermal satisfaction and available consumption capacity. The SA procedure is triggered when a non-zero DA DLMP is observed ($\lambda_k^{DA} > \mathbf{0}$). Indeed, if market conditions remain the same, the RT load flexibility (actual disturbances) is always upper bounded by the robust DA schedule (worst-case disturbances). The SA procedure to obtain demand bids can be outlined as:

At step k, each aggregator (for $DM_i\lambda_k^{DA}) > \mathbf{0}$ independently:

1) Obtains a price sequence Λ by perturbing the λ_k^{DA} from 0 to max(λ_k^{DA}).
2) Finds the optimal consumption ($\mathbf{p}_{i,k}^*(x)$) by solving (17) for $\Lambda(x)$. Repeat this step for all x samples in Λ, creating price schedule pairs ($\mathbf{p}_{i,k}^*(x)$, $\Lambda(x)$).
3) Constructs the demand-bid by fitting a linear curve through all pairs ($\mathbf{p}_{i,k}^*(x)$, $\Lambda(x)$).

For step k, if each LP contracted under aggregator i has a demand bid: $\lambda_k(p_{LP,k}) = mp_{LP,k} + y_0$, then the aggregated demand bid is represented as:

$$\boldsymbol{\lambda}_k(\mathbf{p}_{i,k}) = \mathbf{M}\mathbf{p}_{i,k} + \mathbf{y}_0. \tag{33}$$

In (33), $\mathbf{M}$ and $\mathbf{y}_0$ are the appropriately sized block diagonal matrix and augmented vector, constructed using values of slope m and intercept y_0 from all respective LPs of the aggregator.

2) Maximizing Social Surplus: After collecting demand bids from aggregators, the following optimization problem is solved by the DSO at step k:

$$\max_{\mathbf{p}_{i,k}^*} \sum_{i\in N_i} \frac{1}{2}\mathbf{p}_{i,k}^{\mathbf{T}}\mathbf{M}\mathbf{p}_{i,k} + \mathbf{y}_0^{\mathbf{T}}\mathbf{p}_{i,k} \tag{34a}$$

subject to

$$\mathbf{p}_i^{min} \leq \mathbf{p}_{i,k} \leq \mathbf{p}_i^{max} \tag{34b}$$

$$(\lambda_k^{RT^-}) \; -f_l \leq \sum_{i\in N_i} DM_i\mathbf{p}_{i,k} \leq f_l \; (\lambda_k^{RT^+}) \quad \forall i \in N_i \tag{34c}$$

Within allowable line limits, (34) maximizes the social surplus of the overall system. The LMs $\lambda_k^{RT}(\lambda_k^{RT+} - \lambda_k^{RT-}) \in \mathbb{R}^{n_l}$ are non-zero for the binding constraints (34c). For binding line limits, (34) produces a new price λ_k^{*RT} ($\leq \lambda_k^{*DA}$), increasing the social surplus of the overall system. It is assumed that the maximum $\mathbf{p}_i^{max}$ and minimum $\mathbf{p}_i^{min}$ power in (34b) are inclusive in aggregator demand bids.

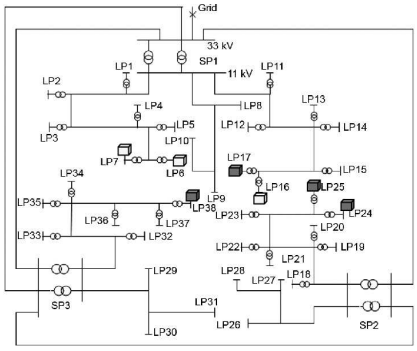

Fig. 5. The modified RBTS distribution network from [43]. Dark and light gray buildings are contracted under aggregator 1 (LP6, 7, 16) and aggregator 2 (LP17, 24, 25, 38), respectively.

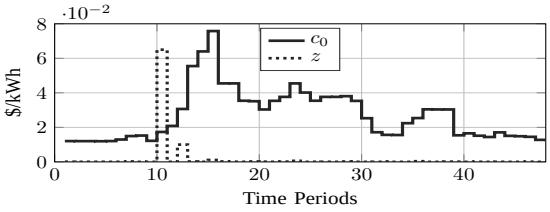

Fig. 6. Energy and reserves prices (temporal resolution 30 minutes) used for conducting simulations.

IV. Simulation Setup and Results

The distributed robust DLMP calculations are evaluated on the Bus 4 Distribution Network of the Roy Billinton Test System (RBTS) [43]. The assumed setup for this paper is presented in Fig. 5. Consistent with the original data [43], 7 commercial LPs are present in the network. Each LP (contracted under an aggregator) is assumed to contain 10 flexible buildings. Each building is modeled considering 10 floors and 10 zones. Each LP is assumed to be operating under a predefined box-constrained disturbance set (see Fig. 2). The simulation parameters are given in Table II. The parameter δ represents the prediction error. The error is calculated as the observed maximum deviation from realized disturbances. For proof of concept, it is assumed that only LP6 and 7 from aggregator 1 are constrained. The energy and reserve prices used for scheduling flexible buildings are shown in Fig. 6. The optimization problems are formulated in YALMIP [44] and solved using CPLEX [45].

Table II
Simulation Setup

δ	Constrained LPs	α_k	Line limits (kW)	β ($/(kWh)^2)
100%	6, 7	0.15	1,350	$1 \cdot 10^{-4}$

In Fig. 7, comparison between the conventional DA DLMP method and the proposed robust distributed method is presented. Both methods are simulated with similar robust constraints i.e. the worst-case disturbance set. The distributed method is terminated when line violation tolerance of 1×10^{-3} MW is reached. In Fig. 7, non-zero DLMPs represent congestion hours. The main causes of congestion are: (1) higher

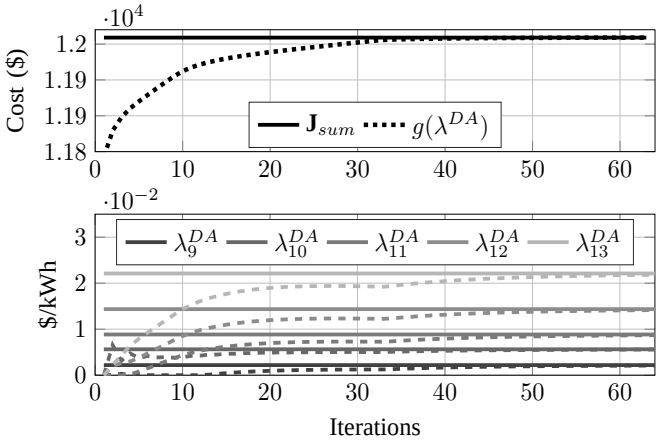

Fig. 7. The comparison between the total cost (top) and DLMPs (bottom) for the proposed distributed and the conventional method. In the bottom plot, solid lines represent conventional DLMPs and dashed lines distributed DLMPs.

space conditioning requirements and (2) reserve placement incentives at time period 10 and 12. Furthermore, it can be observed that the magnitude of DLMPs continue to increase from the time period 9 onwards. This is due to the increase in space conditioning requirements during day time.

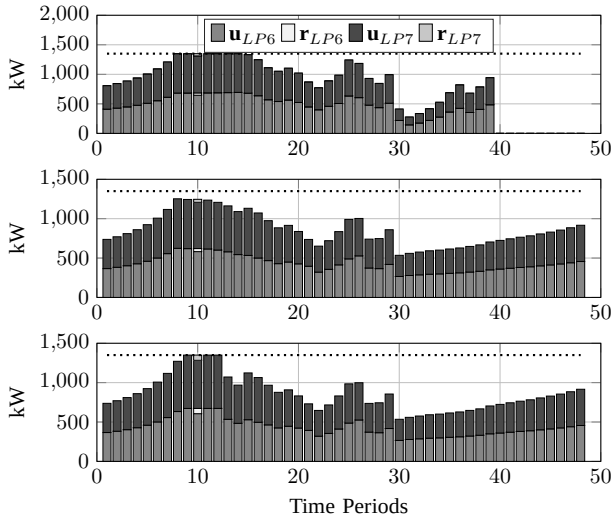

Fig. 8. The robust DA (top), the RT-UA (middle) and the RT-A (bottom). Time period 24 represents exactly the midday.

The RT schedule uses the DA schedule as a reference set point at each step k. For RT operation, receding horizon of 48 periods (1 day) is adopted [7]. In order to compare the effectiveness of the RT adjustment, two RT operations are considered. First, the RT adjusted (RT-A) schedule based on the RT DLMPs using the method described in Section III-B is found. Second, the RT unadjusted (RT-UA) schedule using DA DLMPs is also considered. The comparison of both schedules along with the DA schedule is presented in Fig. 8. It can be seen that the RT-UA schedule is over-constrained, which results in the underutilization of flexible loads. The RT-A schedule removes this under utilization and allows the flexible load to operate much closer to network line limits. Furthermore, during high price periods 13 and 14, compared to the RT-UA case, the RT-A schedules less load. This is because the RT-A schedule utilizes higher flexibility in congested hours, allowing flexible loads to avoid these higher price periods.

The RT-A procedure for the constrained aggregator 1 at time step 10 is elaborated in Fig. 9. Using demand flexibility, it can be observed that aggregator 1 is able to push down the congestion price ($\lambda_{10}^{RT} < \lambda_{10}^{DA}$). This willingness to consume more proves that flexible loads are over-constrained, when operated under unadjusted DA DLMPs. The comparison of

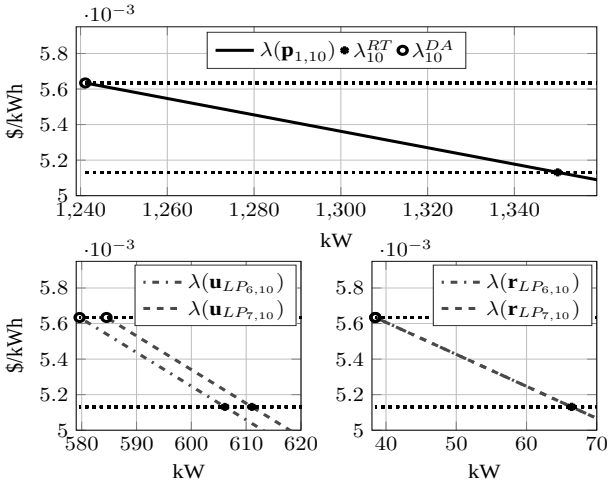

Fig. 9. Real-time adjustment for the aggregator 1 (top), and its LP's energy (bottom left) and reserve procurement (bottom right).

Table III
THE AGGREGATOR 1'S EXPERIENCED LMS

LM ($/MWh)	Time step (k)						
	8	9	10	11	12	13	14
λ_k^{DA}	0.2	2.2	5.6	8.9	14.4	22.1	33.5
λ_k^{RT}	0	1.2	5.1	7.6	12.5	22.1	0

DA LMs with the RT-A LMs for congested time steps is presented in Table III. During congestion time steps k', it can be seen that $\lambda_{k'}^{RT} \leq \lambda_{k'}^{DA}$. This lowering of RT-A LMs improves the overall cost of consumption, as also depicted in Fig. 10. The relative cost improvement (RCI[8]) of 30.2% and 12.7% is observed for the case of RT-A schedule, compared to those of the DA and the RT-UA, respectively. Note that due to the availability of flexibility, loads can consume more in congested hours. This increases the scheduling cost for the RT-A case ($g(1)_{sch}$) by 0.7%, compared to the RT-UA case. However, this increase in the cost gets heavily outweighed by the improvement in the congestion cost ($g(1)_{con}$), which is 94.78% and 69.3%, when compared to the DA and the RT-UA scheduling, respectively.

[8] $(\frac{g(1)^{\text{x}}_{sum} - g(1)^{\text{RT-A}}_{sum}}{g(1)^{\text{RT-A}}_{sum}}) \times 100$, where x is the DA or RT-UA case.

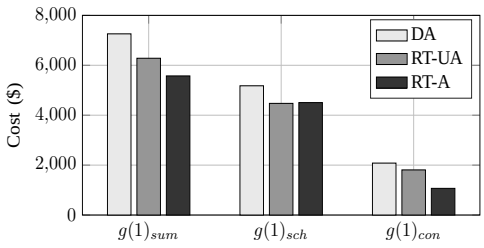

Fig. 10. Aggregator 1's total cost for the DA, RT-A and RT-UA case.

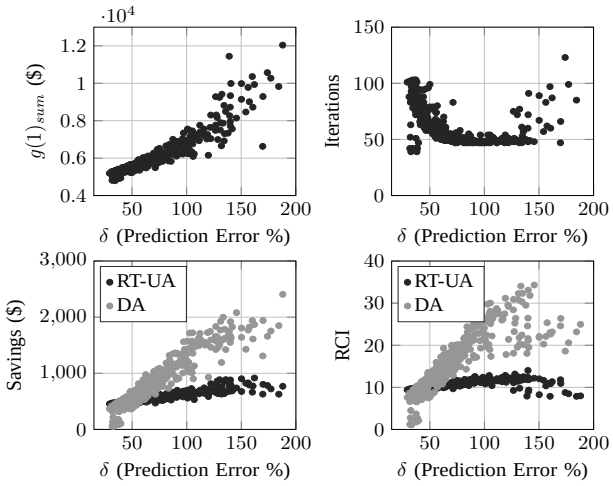

Fig. 11. Number of iterations required to reach the global optimum by the distributed algorithm (top right), the increase in the DA cost (top left), cost savings (bottom left) and the % CI (bottom right) observed with the RT-A, due to the increase in the prediction error.

A. Performance Evaluation

For the same simulation setup, to evaluate the performance of the proposed method, multiple simulations with varying prediction error δ are performed. The results are presented in Fig. 11. It can be observed (top right of Fig. 11) that the number of required iterations for the solution to converge is always less than 150. As expected, the DA scheduling cost (top left of Fig. 11), in order to account for the worst-case disturbance realization, is observed to increase with an increase in the prediction error. Compared to the DA and RT-UA case, the RCI and savings from the RT-A are also presented in Fig. 11. The RCI, compared to the DA case, increases as the prediction error grows, advocating the importance of the RT-A case. However, the RCI from the RT-UA case does not show a large improvement. The first reason is because at higher prediction errors (large DA DLMPs) the accuracy of demand bids is compromised. Hence, these bids may misrepresent the true response of buildings. The second reason is because for both RT operations (the RT-UA and RT-A case) actual disturbances experienced by buildings are considerably smaller than the worst-case disturbances. Hence, by scheduling less consumption, the RT-UA case already somehow compensates the effect of large non zeros DA DLMPs. However, cost saving from the RT-UA case is still observed for the higher δ. To evaluate scalability of the proposed method, 100 runs for various scaled versions of the distribution grid of Fig. 5

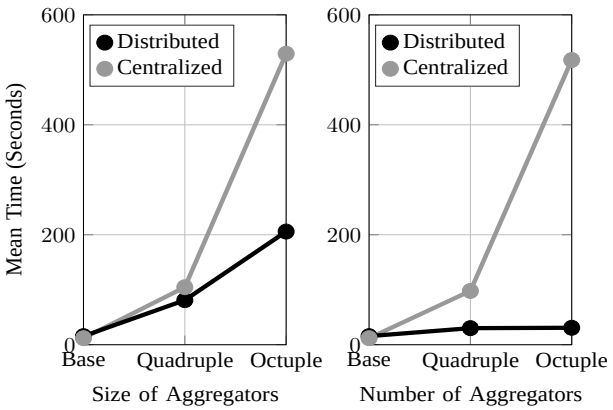

Fig. 12. Comparison of the solution time between distributed and centralized solution. The size (left) and number of aggregators (right) in the distribution grid of Fig. 5 are increased. The base case is given in Table II. For the case of the size of aggregators (left), compared to the base case, quadruple/octuple means an increase in 4/8 times the size of LPs (in kW) contracted by aggregators. For the case of the number of aggregators (right), compared to the base case, quadruple/octuple refers to an increase in 4/8 times the number of aggregators operating in the distribution grid.

are carried out on a 2.4-GHz processor with 64-GB RAM. The mean time needed to compute each scaled scenario is plotted on Fig. 12. Compared to the centralized solution, it can be observed that even with an increase in the size of the distribution grid, the distributed approach has a lower computational time. However, with the increase in the size of aggregators, the computation time also increases. Most notably from Fig. 12, as the same sized number of aggregators increases, the overall solution time drastically improves.[9]

V. Conclusion and Future Work

This paper presents a distributed robust method to alleviate congestion in the presence of flexible buildings in the distribution grid. In particular, a two-step procedure is advocated to increase the overall flexibility of the system. First, DA DLMPs are obtained by incorporating robust load dynamics of buildings and information preservation of aggregators. Second, the RT-A is performed to improve the conservatism of DA robust DLMPs. Compared to previous studies on DLMPs, our proposed method has an improved practical realizability as: (1) it is implementable in a distributed manner, (2) it introduces RT-A to harness the flexibility from loads near RT, and (3) it compliments the combined DA and RT market frameworks, already in place in many power systems. However, to perform the integration of the proposed method into the current power system, more investigations are to be performed. The most notable ones consist of: (1) the interlinking market mechanism between the transmission and distribution system operators, (2) advanced distributed algorithms (such as ADMM) to include non-linear power flows in the DSO problem while improving the solution time and (3) the analysis of demand bids as a function of the receding horizon length and DA DLMPs.

[9]For a fair comparison, an increase in number and size (LPs) of aggregators from the base cases is also accompanied by a proportional increase in line limits of the distribution grids.

VI. Appendix

A. DSO-Aggregator Robust Counterparts

The robust counterpart for the DSO problem is:

$$\min_{\mathbf{p}^*_{i,k}} \sum_{i\in N_i}\sum_{k\in N_t} \mathbf{J}_{sum_{i,k}} \tag{35a}$$

subject to

$$-f_l \le \sum_{i\in N_i}\sum_{k\in N_t} DM_i\mathbf{p}_{i,k} \le f_l \ (\lambda_k^{DA^+}, \lambda_k^{DA^-}) \tag{35b}$$

$$\mathbf{x}^c_{i,k+1} = \mathbf{A}\mathbf{x}^{nc}_{i,k} + \mathbf{B}^c_{\text{agg}}\mathbf{p}_{i,k} + \mathbf{E}\hat{\mathbf{d}}_{i,k} + \boldsymbol{\lambda}^+_{w_{i,k}}\boldsymbol{\sigma}_{i,k} + \boldsymbol{\lambda}^-_{w_{i,k}}\boldsymbol{\sigma}_{i,k} \tag{35c}$$

$$\mathbf{x}^{nc}_{i,k+1} = \mathbf{A}\mathbf{x}^{nc}_{i,k} + \mathbf{B}^{nc}_{\text{agg}}\mathbf{p}_{i,k} + \mathbf{E}\hat{\mathbf{d}}_{i,k} + \boldsymbol{\lambda}^+_{w_{i,k}}\boldsymbol{\sigma}_{i,k} + \boldsymbol{\lambda}^-_{w_{i,k}}\boldsymbol{\sigma}_{i,k} \tag{35d}$$

$$\mathbf{x}^{min}_{i,k} \le \mathbf{x}^c_{i,k} \le \mathbf{x}^{max}_{i,k} \tag{35e}$$

$$\mathbf{x}^{min}_{i,k} \le \mathbf{x}^{nc}_{i,k} \le \mathbf{x}^{max}_{i,k} \tag{35f}$$

$$\mathbf{u}^{min}_{i,k} \le \mathbf{A}^{\text{sum}}\mathbf{p}_{i,k} \le \mathbf{u}^{max}_{i,k} \tag{35g}$$

$$\boldsymbol{\lambda}^+_{w_{i,k}} - \boldsymbol{\lambda}^-_{w_{i,k}} = \mathbf{E} \tag{35h}$$

$$\boldsymbol{\lambda}^+_{w_{i,k}}, \boldsymbol{\lambda}^-_{w_{i,k}}, \mathbf{p}_{i,k}, \mathbf{A}^{\text{diff}}\mathbf{p}_{i,k} \ge \mathbf{0} \qquad \forall i \in N_i, \forall k \in N_t \tag{35i}$$

The robust counterpart of aggregator i is:

$$\min_{\mathbf{p}^*_{i,k}} \sum_{k\in N_t} \lambda^T_{\text{dlmp}_{i,k}}\mathbf{p}_{i,k} + \frac{1}{2}\mathbf{p}^{\mathbf{T}}_{\mathrm{i},k}\mathbf{B}\mathbf{p}_{\mathrm{i},k} \tag{36}$$

subject to

$$(35c) - (35i) \qquad \forall k \in N_t$$

B. Proof for Unique Solution of Robust Counterparts

The Karush Kuhn Tucker (KKT) conditions for the robust counterpart of the DSO problem are:

$$\mathbf{c}_k + \mathbf{B}\mathbf{p}_{i,k} + M_i^T D^T(\lambda_k^{DA^+} - \lambda_k^{DA^-}) + \mathbf{B}^{c^T}_{\text{agg}}\nu^c_{i,k} + \mathbf{B}^{nc^T}_{\text{agg}}\nu^{nc}_{i,k} + \mathbf{A}^{\text{sum}^T}(\mu^{+\text{sum}}_{i,k} - \mu^{-\text{sum}}_{i,k}) - \mathbf{A}^{\text{diff}^T}\mu^{\text{diff}}_{i,k} - \mu^{\mathbf{p}_{i,k}}_{i,k} = \mathbf{0} \tag{37a}$$

$$\lambda_k^{DA^+} \cdot (DM_i\mathbf{p}_{i,k} - f_l) = 0 \tag{37b}$$

$$\lambda_k^{DA^-} \cdot (-DM_i\mathbf{p}_{i,k} - f_l) = 0 \tag{37c}$$

$$\mu^{+\text{sum}}_{i,k} \cdot (\mathbf{A}^{\text{sum}}\mathbf{p}_{i,k} - \mathbf{u}^{max}_{i,k}) = 0 \tag{37d}$$

$$\mu^{-\text{sum}}_{i,k} \cdot (-\mathbf{A}^{\text{sum}}\mathbf{p}_{i,k} + \mathbf{u}^{min}_{i,k}) = 0 \tag{37e}$$

$$\mu^{\text{diff}}_{i,k} \cdot (-\mathbf{A}^{\text{diff}}\mathbf{p}_{i,k}) = 0 \tag{37f}$$

$$\mu^{\mathbf{p}_{i,k}}_{i,k} \cdot (-\mathbf{p}_{i,k}) = 0 \tag{37g}$$

$$\lambda_k^{DA^+}, \lambda_k^{DA^-} \ge 0 \tag{37h}$$

$$\mu^{-\text{sum}}_{i,k}, \mu^{+\text{sum}}_{i,k}, \mu^{\text{diff}}_{i,k}, \mu^{\mathbf{p}_{i,k}}_{i,k} \ge 0 \tag{37i}$$

$$(35b) - (35i) \qquad \forall i \in N_i, \forall k \in N_t \tag{37j}$$

Similarly, the KKT conditions for the robust i^{th} aggregator is:

$$\mathbf{c}_k + \mathbf{B}\mathbf{p}_{i,k} + M_i^T D^T(\lambda_k^{DA^+} - \lambda_k^{DA^-}) + \mathbf{B}^{c^T}_{\text{agg}}\nu^c_{i,k} + \mathbf{B}^{nc^T}_{\text{agg}}\nu^{nc}_{i,k} + \mathbf{A}^{\text{sum}^T}(\mu^{+\text{sum}}_{i,k} - \mu^{-\text{sum}}_{i,k}) - \mathbf{A}^{\text{diff}^T}\mu^{\text{diff}}_{i,k} - \mu^{\mathbf{p}_{i,k}}_{i,k} = \mathbf{0} \tag{38a}$$

$$\mu^{-\text{sum}}_{i,k} \cdot (\mathbf{A}^{\text{sum}}\mathbf{p}_{i,k} - \mathbf{u}^{max}_{i,k}) = 0 \tag{38b}$$

$$\mu^{-\text{sum}}_{i,k} \cdot (-\mathbf{A}^{\text{sum}}\mathbf{p}_{i,k} + \mathbf{u}^{min}_{i,k}) = 0 \tag{38c}$$

$$\mu^{\text{diff}}_{i,k} \cdot (-\mathbf{A}^{\text{diff}}\mathbf{p}_{i,k}) = 0 \tag{38d}$$

$$\mu^{\mathbf{p}_{i,k}}_{i,k} \cdot (-\mathbf{p}_{i,k}) = 0 \tag{38e}$$

$$(35c) - (35i), (37i) \qquad \forall k \in N_t \tag{38f}$$

It can be observed that the robust DSO problem (35) has a quadratic cost function and affine constraints. Furthermore, the Hessian matrix of the quadratic cost is a positive definite matrix. This makes the robust DSO problem a strictly convex QP. Hence, its KKT conditions are necessary and sufficient, and for a feasible problem the achieved solution is unique [41]. The robust aggregator i problem follows similar arguments. If the solution of the KKT conditions (37) of the robust DSO problem is given as:
$(\mathbf{p}^*_{i,k},\ \mu^{-\text{sum}*}_{i,k},\ \mu^{+\text{sum}*}_{i,k},\ \mu^{\text{diff}*}_{i,k},\ \mu^{\mathbf{p}_{i,k}*}_{i,k},\ \nu^{c*}_{i,k},\ \nu^{nc*}_{i,k},\ \lambda_k^{DA^+*},\ \lambda_k^{DA^-*})$. Then by comparison, this solution also satisfies the KKT conditions of the robust i^{th} aggregator (38). This is because the robust aggregator constraints are also contained within the KKT conditions of the DSO problem. Hence, any solution which satisfies the robust DSO problem is also a valid solution for the robust aggregator problem. But the solution of the robust aggregator problem may not be a valid solution for the robust DSO problem. This is because aggregator i does not include line limits constraints of the robust DSO problem [(37b), (37c)]. However, it can be observed that due to the robust DSO and aggregator problems being strictly convex, the obtained solution must be unique. Hence, this uniqueness enforces that any solution of the robust aggregator problem must also be the solution of the robust DSO problem. However, it must be noted here that due to the deployment of the worst-case disturbance bounds, this unique solution is optimal for the worst-case and feasible for any other disturbance realization.

C. Coupling Constraint and Dual Decomposition

Consider a simplified version of the Lagrangian described in (24), containing only two aggregators along with local temperature and power limitations:

$$\begin{aligned} L = &-\lambda_k^{DA^T} f_l + \mathbf{J}_{sum_{1,k}} + \lambda_k^{DA^T} DM_1\mathbf{p}_{1,k} \\ &+\nu^T_{1,k}(-\mathbf{x}_{1,k+1} + \mathbf{A}\mathbf{x}_{1,k} + \mathbf{B}_{\text{agg}}\mathbf{p}_{1,k} + \mathbf{E}\hat{\mathbf{d}}_{1,k} \\ &+\boldsymbol{\lambda}^+_{w_{1,k}}\boldsymbol{\sigma}_{1,k} + \boldsymbol{\lambda}^-_{w_{1,k}}\boldsymbol{\sigma}_{1,k}) + \mu^T_{1,k}(\mathbf{A}^{\text{sum}}\mathbf{p}_{1,k} - \mathbf{u}^{max}_{1,k}) \\ &+\mathbf{J}_{sum_{2,k}} + \lambda_k^{DA^T} DM_2\mathbf{p}_{2,k} \\ &+\nu^T_{2,k}(-\mathbf{x}_{2,k+1} + \mathbf{A}\mathbf{x}_{2,k} + \mathbf{B}_{\text{agg}}\mathbf{p}_{2,k} + \mathbf{E}\hat{\mathbf{d}}_{2,k} \\ &+\boldsymbol{\lambda}^+_{w_{2,k}}\boldsymbol{\sigma}_{2,k} + \boldsymbol{\lambda}^-_{w_{2,k}}\boldsymbol{\sigma}_{2,k}) + \mu^T_{2,k}(\mathbf{A}^{\text{sum}}\mathbf{p}_{2,k} - \mathbf{u}^{max}_{2,k}) \end{aligned}$$

The above Lagrangian demonstrates how the DSO's coupling constraint (14b) splits among aggregators. Essentially, for aggregator i, matrices M_i (node mapping) and D (PTDF) translate power consumption of aggregators to the line flow in distribution grid. In the end, individual contributions of each aggregator is summed up ($DM_i\mathbf{p}_{i,k}$) to obtain the total line flows in the distribution grid. Note that this is the only coupling in the above Lagrangian. For a given coupling dual λ_k^{DA}, the above presented Lagrangian can be equivalently written as solving the following local robust aggregator problems [42]:

$$g_1(\lambda_k^{DA}) = \min_{\mathbf{p}^*_{1,k}} \ \mathbf{J}_{sum_{1,k}} + \lambda_k^{DA^T} DM_1\mathbf{p}_{1,k}$$
$$\text{s.t.} \quad \text{Aggregator 1's energy requirements} \tag{40}$$

$$g_2(\lambda_k^{DA}) = \min_{\mathbf{p}^*_{2,k}} \ \mathbf{J}_{sum_{2,k}} + \lambda_k^{DA^T} DM_2\mathbf{p}_{2,k}$$
$$\text{s.t.} \quad \text{Aggregator 2's energy requirements} \tag{41}$$

and then iterating (it) between aggregators (42a) and the DSO (42b), until the convergence is achieved.

$$\mathbf{p}_{1,k}^{*^{it}} = g1(\lambda_k^{DA^{it}}), \quad \mathbf{p}_{2,k}^{*^{it}} = g2(\lambda_k^{DA^{it}}) \tag{42a}$$

$$\lambda_k^{DA^{it+1}} = (\lambda_k^{DA^{it}} + \alpha h^{it})_+ \tag{42b}$$

In (42), if $g(\lambda_k^{DA^{it}}) = g_1(\lambda_k^{DA^{it}}) + g_2(\lambda_k^{DA^{it}})$ then $h \in \partial(-g)(\lambda_k^{DA^{it}}) = DM_1\mathbf{p}_{1,k}^{*^{it}} + DM_2\mathbf{p}_{2,k}^{*^{it}} - f_l$, where $\mathbf{p}_{1,k}^{*^{it}}$ and $\mathbf{p}_{2,k}^{*^{it}}$ are solutions of (40) and (41) respectively.

The first observation from the above mentioned method is that $g(\lambda_k^{DA})$ is differentiable, hence only one element exists in its subdifferential [46]. Differentiability also implies that a constant small enough step size α will yield convergence [46]. For the case of our strictly convex problems (QP), this means that we can recover a unique global solution of the whole problem (see Section VI-B). The second observation is that aggregators [(40), (41)] handle uncertainties locally. Since uncertainty sets are predefined in each robust aggregator problem, the iterative link between aggregators and the DSO, through global LM λ_k^{DA} does not contain any uncertainty.

For two aggregators and two time steps $(k = 1, 2)$, Fig. 13 and Fig. 14 show the progress of dual decomposition-based subgradient method. For each iteration, aggregators incorporate $\lambda_k^{DA^{it}}$ to find their local robust solutions $\mathbf{p}_{1,k}^{it}, \mathbf{p}_{2,k}^{it}$. These local solutions, when infeasible for the overall DSO problem, propagate through the projected subgradient method. This method moves the local robust solutions in the direction of its negative subgradient, until they converge to a unique solution.

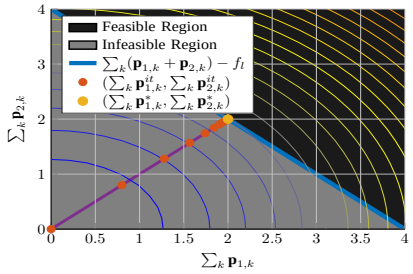

Fig. 13. Visualization of dual decomposition-based subgradient method on a small QP example. This example represents combined energy requirements for aggregators, $0 \leq \sum_k (\mathbf{p}_{1,k} + \mathbf{p}_{2,k}) \leq 4$ and the quadratic cost function, $\sum_k (\mathbf{p}_{1,k}^2 + \mathbf{p}_{2,k}^2)$. Trivially, the minimum of this problem is zero energy requirements for both aggregator $[\forall k, \mathbf{p}_{1,k}, \mathbf{p}_{2,k} = 0]$. Hence, coupling constraint, $\sum_k(\mathbf{p}_{1,k} + \mathbf{p}_{2,k}) \geq 4$ is introduced.

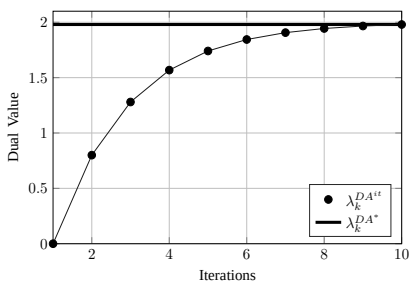

Fig. 14. Dual variable updates for the subgradient method of Fig. 13.

REFERENCES

[1] M. Maasoumy, "Controlling Energy-Efficient Buildings in the Context of Smart Grid: A Cyber Physical System Approach," Ph.D. dissertation, University of California, Berkeley, 2013. [Online]. Available: http://www.eecs.berkeley.edu/Pubs/TechRpts/2013/EECS-2013-244.html

[2] D. B. Crawley, J. W. Hand, M. Kummert, and B. T. Griffith, "Contrasting the capabilities of building energy performance simulation programs," *Building and Environment*, vol. 43, no. 4, pp. 661–673, apr 2008.

[3] F. Oldewurtel, A. Parisio, C. N. Jones, D. Gyalistras, M. Gwerder, V. Stauch, B. Lehmann, and M. Morari, "Use of model predictive control and weather forecasts for energy efficient building climate control," *Energy and Buildings*, vol. 45, pp. 15–27, feb 2012.

[4] Y. Ma, F. Borrelli, B. Hencey, B. Coffey, S. Bengea, and P. Haves, "Model Predictive Control for the Operation of Building Cooling Systems," *IEEE Transactions on Control Systems Technology*, vol. 20, no. 3, pp. 796–803, 2012.

[5] E. Vrettos, F. Oldewurtel, and G. Andersson, "Robust Energy-Constrained Frequency Reserves From Aggregations of Commercial Buildings," *IEEE Transactions on Power Systems*, pp. 1–14, 2016.

[6] E. Vrettos and G. Andersson, "Scheduling and Provision of Secondary Frequency Reserves by Aggregations of Commercial Buildings," *IEEE Transactions on Sustainable Energy*, vol. 7, no. 2, pp. 850–864, 2016.

[7] S. Hanif, D. Fernando, M. Maasoumy, T. Massier, T. Hamacher, and T. Reindl, "Model predictive control scheme for investigating demand side flexibility in Singapore," in *2015 50th International Universities Power Engineering Conference (UPEC)*, 2015, pp. 1–6.

[8] S. Hanif, C. Gruentgens, T. Massier, T. Hamacher, and T. Reindl, "Quantifying the effect on the load shifting potential of buildings due to ancillary service provision," in *2016 IEEE Power and Energy Society General Meeting (PESGM)*. IEEE, jul 2016, pp. 1–5.

[9] S. Hanif, D. F. R. Melo, M. Maasoumy, T. Massier, T. Hamacher, and T. Reindl, "Robust reserve capacity provision and peak load reduction from buildings in smart grids," in *2016 IEEE Power and Energy Society General Meeting (PESGM)*, jul 2016, pp. 1–5.

[10] S. Hanif, T. Massier, H. B. Gooi, T. Hamacher, and T. Reindl, "Cost Optimal Integration of Flexible Buildings in Congested Distribution Grids," *IEEE Transactions on Power Systems*, pp. 1–1, 2016.

[11] R. Verzijlbergh, L. J. De Vries, and Z. Lukszo, "Renewable Energy Sources and Responsive Demand. Do We Need Congestion Management in the Distribution Grid?" *IEEE Transactions on Power Systems*, vol. 29, no. 5, pp. 2119–2128, 2014.

[12] P. Bach Andersen, J. Hu, and K. Heussen, "Coordination strategies for distribution grid congestion management in a multi-actor, multi-objective setting," *IEEE PES Innovative Smart Grid Technologies Conference Europe*, pp. 1–8, 2012.

[13] S. Huang, Q. Wu, Z. Liu, and A. H. Nielsen, "Review of Congestion Management Methods for Distribution Networks with High Penetration of Distributed Energy Resources," *5th IEEE PES Innovative Smart Grid Technologies Europe (ISGT Europe)*, 2014.

[14] N. O'Connell, Q. Wu, J. Østergaard, A. H. Nielsen, S. T. Cha, and Y. Ding, "Day-ahead tariffs for the alleviation of distribution grid congestion from electric vehicles," *Electric Power Systems Research*, vol. 92, pp. 106–114, nov 2012.

[15] R. Li, Q. Wu, and S. S. Oren, "Distribution Locational Marginal Pricing for Optimal Electric Vehicle Charging Management," *IEEE Transactions on Power Systems*, vol. 29, no. 1, pp. 203–211, jan 2014.

[16] S. Huang, Q. Wu, S. S. Oren, R. Li, and Z. Liu, "Distribution Locational Marginal Pricing Through Quadratic Programming for Congestion Management in Distribution Networks," *IEEE Transactions on Power Systems*, vol. 30, no. 4, pp. 2170–2178, jul 2015.

[17] S. Huang, Q. Wu, L. Cheng, Z. Liu, and H. Zhao, "Uncertainty Management of Dynamic Tariff Method for Congestion Management in Distribution Networks," *IEEE Transactions on Power Systems*, pp. 1–8, 2016.

[18] M. Maasoumy and A. Sangiovanni-Vincentelli, "Optimal Control of Building HVAC Systems in the Presence of Imperfect Predictions," in *ASME 2012 5th Annual Dynamic Systems and Control Conference*, 2012.

[19] J. M. Morales, A. J. Conejo, H. Madsen, P. Pinson, and M. Zugno, *Integrating Renewables in Electricity Markets*, ser. International Series in Operations Research & Management Science. Boston, MA: Springer US, 2014, vol. 205.

[20] S. E. Widergren, K. Subbarao, J. C. Fuller, D. P. Chassin, A. Somani, M. C. Marinovici, and J. L. Hammerstrom, "AEP Ohio gridSMART demonstration project real-time pricing demonstration analysis," Pacific Northwest National Laboratory, Tech. Rep. February, 2014.

[21] D. J. Hammerstrom, R. Ambrosio, T. a. Carlon, J. G. Desteese, R. Kajfasz, R. G. Pratt, and D. P. Chassin, "Pacific Northwest GridWise(TM) Testbed Demonstration Projects Part I . Olympic Peninsula Project," Pacific Northwest National Laboratory, Tech. Rep., 2007.
[22] J. Baillieul, M. C. Caramanis, and M. D. Ilic, "Control Challenges in Microgrids and the Role of Energy-Efficient Buildings," *Proceedings of the IEEE*, vol. 104, no. 4, pp. 692–696, apr 2016.
[23] J.-Y. Joo and M. D. Ilic, "An Information Exchange Framework Utilizing Smart Buildings for Efficient Microgrid Operation," *Proceedings of the IEEE*, vol. 104, no. 4, pp. 858–864, apr 2016.
[24] T. Samad, E. Koch, and P. Stluka, "Automated Demand Response for Smart Buildings and Microgrids: The State of the Practice and Research Challenges," *Proceedings of the IEEE*, vol. 104, no. 4, pp. 726–744, 2016.
[25] M. Caramanis, E. Ntakou, W. W. Hogan, A. Chakrabortty, and J. Schoene, "Co-optimization of power and reserves in dynamic T&D power markets with nondispatchable renewable generation and distributed energy resources," *Proceedings of the IEEE*, vol. 104, no. 4, pp. 807–836, 2016.
[26] E. Loukarakis, C. J. Dent, and J. W. Bialek, "Decentralized multi-period economic dispatch for real-time flexible demand management," *IEEE Transactions on Power Systems*, vol. 31, no. 1, pp. 672–684, 2016.
[27] E. Loukarakis, J. W. Bialek, and C. J. Dent, "Investigation of Maximum Possible OPF Problem Decomposition Degree for Decentralized Energy Markets," *IEEE Transactions on Power Systems*, vol. 30, no. 5, pp. 2566–2578, 2015.
[28] M. Kraning, E. Chu, J. Lavaei, and S. Boyd, "Message Passing for Dynamic Network Energy Management," *Foundations and Trends in Optimization*, vol. 1, no. 2, pp. 70–122, 2014.
[29] J.-Y. Joo and M. D. Ilic, "Multi-Layered Optimization Of Demand Resources Using Lagrange Dual Decomposition," *IEEE Transactions on Smart Grid*, vol. 4, no. 4, pp. 2081–2088, dec 2013.
[30] Y. Zhang and G. B. Giannakis, "Distributed Stochastic Market Clearing With High-Penetration Wind Power," *IEEE Transactions on Power Systems*, vol. 31, no. 2, pp. 895–906, mar 2016.
[31] N. Gatsis and G. B. Giannakis, "Decomposition algorithms for market clearing with large-scale demand response," *IEEE Transactions on Smart Grid*, vol. 4, no. 4, pp. 1976–1987, 2013.
[32] S. Boyd, N. Parikh, B. P. E Chu, and J. Eckstein, "Distributed Optimization and Statistical Learning via the Alternating Direction Method of Multipliers," *Foundations and Trends in Machine Learning*, vol. 3, no. 1, pp. 1–122, 2011.
[33] M. Maasoumy, A. Pinto, and A. Sangiovanni-Vincentelli, "Model-Based Hierarchical Optimal Control Design for HVAC Systems," in *ASME 2011 Dynamic Systems and Control Conference*, 2011, pp. 271–278.
[34] D. Sturzenegger, V. Semeraro, D. Gyalistras, and R. S. Smith, "Building Resistance-Capacitance Modeling (BRCM) ToolBox," 2012. [Online]. Available: http://www.brcm.ethz.ch
[35] D. Sturzenegger, D. Gyalistras, M. Morari, and R. S. Smith, "Model Predictive Climate Control of a Swiss Office Building: Implementation, Results, and Cost-Benefit Analysis," *IEEE Transactions on Control Systems Technology*, vol. 24, no. 1, pp. 1–12, 2016.
[36] S. Chatzivasileiadis, M. Bonvini, J. Matanza, R. Yin, T. S. Nouidui, E. C. Kara, R. Parmar, D. Lorenzetti, M. Wetter, and S. Kiliccote, "Cyber-physical modeling of distributed resources for distribution system operations," *Proceedings of the IEEE*, vol. 104, no. 4, pp. 789–806, 2016.
[37] S. Swan, "Interruptible load: new partnerships for better energy management," *2005 International Power Engineering Conference*, pp. 888–892 Vol. 2, 2005.
[38] Energy Market Authority, "Implementing Demand Response In The National Electricity Market of Singapore," EMA, Singapore, Tech. Rep., 2013. [Online]. Available: http://tinyurl.com/zw5lmsn
[39] ——, "Introduction to the National Electricity Market," Energy Market Authority, Singapore, Tech. Rep. October, 2010. [Online]. Available: http://tinyurl.com/j36eagv
[40] "Energy Market Company Singapore." [Online]. Available: https://www.emcsg.com/
[41] L. Boyd, Stephen and Vandenberghe, *Convex optimization theory*. Cambridge University Press, 2004.
[42] S. Boyd, L. Xiao, A. Mutapcic, and J. Mattingley, "Notes on Decomposition Methods," Stanford University, Tech. Rep., 2008.
[43] R. Allan, R. Billinton, I. Sjarief, L. Goel, and K. So, "A reliability test system for educational purposes-basic distribution system data and results," *IEEE Transactions on Power Systems*, vol. 6, no. 2, pp. 813–820, may 1991.
[44] J. Loefberg, "YALMIP: A toolbox for Modeling and Optimization in MATLAB," in *CACSD Conference*, Taipei, 2004.
[45] IBM, "IBM ILOG CPLEX Optimization Studio." [Online]. Available: http://www-03.ibm.com/software/products/en/ibmilogcpleoptistud
[46] S. Boyd, L. Xiao, and A. Mutapcic, "Subgradient methods," *lecture notes of EE392o, Stanford*, vol. 1, no. May, pp. 1–21, 2003. [Online]. Available: goo.gl/S0KX0W

Sarmad Hanif (S'15) received B.Sc. in Electrical Engineering from the University of Engineering and Technology Lahore, Pakistan and M.Sc. in Power Engineering from the Technical University of Munich (TUM), Germany in 2009 and 2013, respectively. Since June 2014, he is pursuing Ph.D. at the Technical University of Munich (TUM), Germany. He is interested in the integration of cost effective and reliable flexible demand into power systems.

H. B. Gooi (SM'95) received the B.S. degree in EE from National Taiwan University in 1978; the M.S. degree in EE from the University of New Brunswick in 1980; and the Ph.D. degree in EE from Ohio State University in 1983. From 1983 to 1985, he was an Assistant Professor with Lafayette College, Easton. From 1985 to 1991, he was a Senior Engineer with Empros (now Siemens), Minneapolis, where he was responsible for the design and testing coordination of domestic and international energy management system projects. In 1991, he joined the School of Electrical and Electronic Engineering, Nanyang Technological University, Singapore, as a Senior Lecturer, where he has been an Associate Professor since 1999. He was the Deputy Head of Power Engineering Division during 2008-2014. He has been an Editor of IEEE Transactions on Power Systems since 2016. His current research interests include microgrid energy management systems dealing with storage, renewable energy sources, electricity market and spinning reserve.

Tobias Massier (M'15) received the Dipl.-Ing. and PhD degree in electrical engineering and information technology from the Technical University of Munich (TUM), Germany, in 2002 and 2010 respectively. From 2009 to 2012, he managed a new Master Program in Power Engineering at TUM. Since 2013, he has been with TUM CREATE as Principal Investigator of the research group Electrification Suite and Test Lab. His research interests are in transportation electrification, vehicle emissions and integration of renewable energies.

Thomas Hamacher is a full professor in renewable and sustainable energy systems at the Technical University Munich (TUM), Germany. His research focuses on energy and systems analysis, focusing on urban energy systems, the integration of renewable energy into the power grid, and innovative nuclear systems (including fusion). Other focuses of his work are the methods and fundamentals of energy models.

Thomas Reindl is the Deputy CEO of the Solar Energy Research Institute of Singapore (SERIS) and a Principal Research Fellow (equivalent to Associate Professor) at the National University of Singapore (NUS). Before joining SERIS, Dr. Reindl held several management positions within the solar industry. Dr. Reindl holds a Master in Chemistry, a Ph.D. in Natural Sciences and an MBA from INSEAD, all awarded with the highest honours. In addition to his appointment as Deputy CEO of the institute, he is also Director of the Solar Energy Systems cluster at SERIS since 2010.